

Disentangling sources of quantum entanglement in quench dynamics

Lorenzo Pastori,¹ Markus Heyl,² and Jan Carl Budich¹¹*Institute of Theoretical Physics, Technische Universität Dresden, 01062 Dresden, Germany*²*Max-Planck-Institut für Physik komplexer Systeme, Nöthnitzer Straße 38, 01187 Dresden, Germany*

(Received 15 May 2019; published 14 August 2019)

Quantum entanglement may have various origins ranging from solely interaction-driven quantum correlations to single-particle effects. Here, we explore the dependence of entanglement on time-dependent single-particle basis transformations in fermionic quantum many-body systems, thus aiming at isolating single-particle sources of entanglement growth in quench dynamics. Using exact diagonalization methods, for paradigmatic nonintegrable models we compare to the standard real-space cut various physically motivated bipartitions. Moreover, we search for a minimal entanglement basis using local optimization algorithms, which at short to intermediate postquench times yields a significant reduction of entanglement beyond a dynamical Hartree-Fock solution. In the long-time limit, we identify an asymptotic universality of entanglement for weakly interacting systems, as well as a crossover from dominant real-space to momentum-space entanglement in Hubbard models undergoing an interaction quench. Finally, we discuss the relevance of our findings for the development of tensor-network-based algorithms for quantum dynamics.

DOI: [10.1103/PhysRevResearch.1.012007](https://doi.org/10.1103/PhysRevResearch.1.012007)

Entanglement as one of the most fundamental traits of quantum mechanics plays a key role in various physical contexts, ranging from the characterization of complex many-body states [1,2] to its use as a resource for quantum technologies [3–7]. On the other hand, strong entanglement in correlated quantum matter poses a significant challenge that limits both its analytical and numerical description. This becomes particularly relevant in nonequilibrium dynamics, where entanglement generically grows rapidly with time [8–23]. This growth, however, may originate from mechanisms of different inherent complexity: While it can already be found in analytically solvable free theories, at the opposite end entanglement can be purely interaction induced. Yet, it has remained largely unexplored as to what extent a heterogeneous dynamical entanglement content may be distinguished according to its various sources on general grounds.

The purpose of this Rapid Communication is to investigate how the single-particle content of entanglement in quantum quench dynamics can be isolated from genuine many-body complexity, thereby revealing physically distinct sources of quantum correlations. To this end, we study the dependence on generally *time-dependent* single-particle basis rotations (entanglement cuts) of the half-system entanglement entropy

$$S(t) = -\text{tr}[\rho_{A_t} \log(\rho_{A_t})], \quad (1)$$

where $\rho_{A_t} = \text{tr}_{B_t} \rho$ denotes the reduced density matrix of subsystem A_t at time t obtained from the full density matrix $\rho = |\psi(t)\rangle\langle\psi(t)|$ by tracing out its complement B_t [see Fig. 1(a)],

and $|\psi(t)\rangle$ is the state of the system at time t . Going beyond the conventionally used real- or momentum-space basis, we investigate different choices of single-particle orbitals for the bipartition of the system in A_t and B_t , including physically motivated states such as dispersing Wannier orbitals or time-dependent Hartree-Fock solutions. Furthermore, we search for an optimal (i.e., yielding minimal entanglement S) orbital basis using local optimization algorithms [see the inset in Fig. 1(b)], in order to separate genuine many-body entanglement content, originating from quantum correlations involving several particles, from single-particle contributions.

As we exemplify for several nonintegrable fermionic quantum many-body systems, for quite long transient times the entanglement entropy indeed exhibits a significant basis dependence [see Fig. 1(b)]. Based on our concrete case studies in the framework of exact diagonalization, in this context we identify several general principles for both transient and asymptotically long times, including (i) an asymptotic universality (in the sense of basis independence) of entanglement in band insulators with weak to modest interactions, and (ii) a crossover between real-space and momentum-space entanglement in Hubbard models undergoing an interaction quench. Our results contribute towards the physical understanding of entanglement in complex quantum matter, and might be of key relevance for the development of numerical algorithms for quantum dynamics based on tensor-network approaches [24–37], whose efficiency crucially depends on entanglement scaling.

Entanglement dynamics from Krylov time propagation. For our quantitative study, we consider a system of n_p interacting fermions on a lattice with sites $j = 1, \dots, L$, which are annihilated by the vector of field operators $c = (c_1, \dots, c_L)$. To quench the system out of equilibrium, the Hamiltonian is suddenly changed from H_i to H_f at time $t = 0$, assuming that the many-body state $|\psi(t = 0)\rangle$ was prepared as the ground

Published by the American Physical Society under the terms of the [Creative Commons Attribution 4.0 International](https://creativecommons.org/licenses/by/4.0/) license. Further distribution of this work must maintain attribution to the author(s) and the published article's title, journal citation, and DOI.

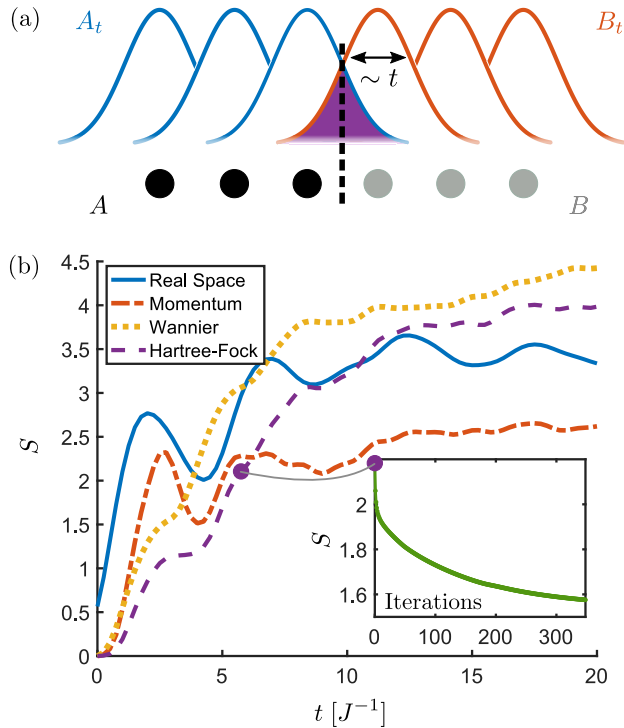


FIG. 1. (a) Illustration of a time-dependent entanglement cut A_t/B_t corresponding to a basis of dispersing Wannier orbitals, in comparison to a standard real-space cut A/B . (b) Time dependence of the entanglement entropy S of the interacting model defined in Eqs. (4) and (5) far from equilibrium. Different curves correspond to different entanglement cuts (see plot legend). Inset: Basis optimization of entanglement beyond the dynamical Hartree-Fock cut. Parameters are $L = 24$, $n_p = 12$, $U = J = 1.0$, $W = 0$, $m_i = 1.8$, $m_f = 0.2$.

state of H_i at $t < 0$. Using numerically exact Krylov time-propagation methods [38,39], for several examples of H_i and H_f representing quenches into nonintegrable systems, we then compute the time-evolved wave function ($\hbar = 1$)

$$|\psi(t)\rangle = e^{-iH_f t} |\psi(0)\rangle. \quad (2)$$

In order to study the dynamics of the (von Neumann) entanglement entropy $S(t)$, we decompose the system into two subsystems, A_t and B_t , each containing $L/2$ orbitals and on average $n_p/2$ particles. However, we do not restrict this decomposition (entanglement cut) to the real-space lattice space, but consider time-dependent basis orbitals $\tilde{c}_t = u_t c$, resulting from the real-space lattice representation by an arbitrary $U(L)$ transformation u_t [with $U(L)$ denoting the group of $L \times L$ unitary matrices].

To represent the time-evolved wave function in an arbitrary orbital basis, we need to express u_t in many-body Hilbert space, where it is denoted by U_t .

Naively applying U_t to the real-space representation $\psi(t)$ of the state vector $|\psi(t)\rangle$ would generate an unfeasible computational cost $\sim N^2$, where N is the dimension of the many-body Hilbert space of n_p particles.

However, exploiting that U_t formally may be seen as a “time evolution” with respect to the free Hamiltonian

$$\tilde{H}_t = \sum_{j,\ell} (i \log u_t)_{j,\ell} c_j^\dagger c_\ell \text{ yields}$$

$$\tilde{\psi}(t) = U_t \psi(t) = e^{-i\tilde{H}_t} \psi(t), \quad (3)$$

which naturally allows for the efficient [$O(N)$] computation of the transformed representation $\tilde{\psi}(t)$, again using Krylov time propagation with respect to the fictitious Hamiltonian \tilde{H} .

In the following, we present exact numerical data on the quench dynamics of systems with up to $L = 24$ sites and $n_p = 12$ fermions, where $N \approx 2.7 \times 10^6$. Concretely, we study two examples of nonintegrable ergodic model systems, (i) a one-dimensional (1D) two-band band insulator that is quenched to a topological insulator (TI) phase with weak to modest interactions, and (ii) a metallic single-band Fermi-Hubbard model with next-nearest-neighbor (NNN) interactions. By comparison of these physically quite different scenarios, we will identify various features relating to the basis dependence of entanglement in quantum quench dynamics.

(i) *Weakly interacting topological insulator.* We first discuss a one-dimensional (1D) two-banded system similar to the celebrated Su, Schrieffer, and Heeger (SSH) model [40,41]. There, the lattice index $j = 1, \dots, L$ is decomposed into a unit-cell index $i = 1, \dots, L/2$ and a sublattice index $\alpha = a, b$ such that $j = 2i - 1$ for site a in cell i and $j = 2i$ for site b in cell i , respectively. In reciprocal space, the two-band Bloch Hamiltonian at lattice momentum $k = 4\pi p/L$, $p = 0, \dots, L/2 - 1$ of the system is defined as

$$h(k) = [m(t) + J \cos(k)]\sigma_x + J \sin(k)\sigma_y, \quad (4)$$

where σ_i are the standard Pauli matrices acting on a/b sublattice space, $m(t)$ plays the role of a Dirac mass parameter that is quenched from m_i to m_f at $t = 0$, and J is the hopping strength between neighboring unit cells. For $|m| < |J|$, the model is in a topological insulator phase protected by the chiral symmetry $\sigma_z h(k) \sigma_z = -h(k)$, while at $|m| = |J|$ a topological quantum phase transition to a trivial band insulator phase extending over the parameter regime $|m| > |J|$ occurs. Here, we focus on quenches which change the topological phase of the system Hamiltonian, by choosing m_i in the trivial and m_f in the nontrivial phase, respectively.

For the (standard) real-space entanglement cut, even the noninteracting system is found to exhibit linear entanglement growth at small times. However, this entanglement is readily seen to be entirely basis dependent: The exact solution $|\psi(t)\rangle$ stays a single Slater determinant at all times, leading to zero entanglement in a suitable basis obtained from time-evolved Wannier functions or Bloch functions representing the initial uncorrelated state. This provides a conceptually simple example for how strongly the entanglement of a system far from equilibrium may depend on the chosen representation.

We now address the natural question as to how an integrability breaking interaction term affects this phenomenology. To this end, we add to the free model (4) the interaction Hamiltonian

$$H_I = \sum_i [U n_{i,a} n_{i,b} + W (n_{i,a} n_{i+1,b} + n_{i,b} n_{i+1,a})], \quad (5)$$

with $n_{i,\alpha} = c_{i,\alpha}^\dagger c_{i,\alpha}$ ($\alpha = a, b$), where already a nonzero U or W individually is sufficient to make the model nonintegrable, and both terms preserve the protecting chiral symmetry.

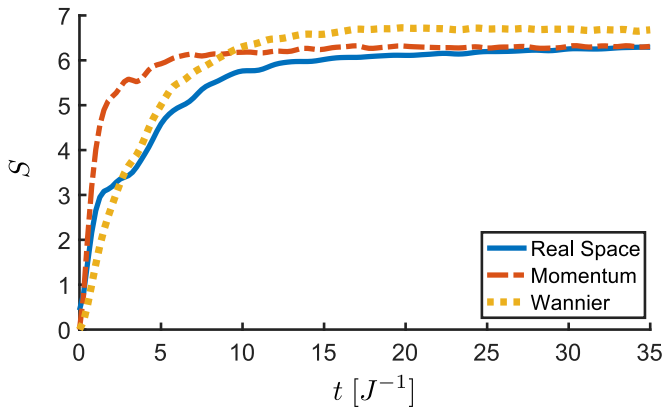


FIG. 2. Asymptotic universality of the entanglement entropy S of the equilibrating quenched interacting topological insulator model defined in Eqs. (4) and (5): Different curves corresponding to different entanglement cuts (see plot legend) saturate to similar values at long times. Parameters: $L = 24$, $n_p = 12$, $W = J = 1.0$, $U = 0$, $m_i = 1.8$, $m_f = 0.2$.

We first discuss the case on $U = J$, $W = 0$ for transient times [see Fig. 1(b)]. For the Bloch and Wannier entanglement cut, in which the noninteracting solution would exhibit zero entanglement, S is lower than in the real-space cut, for short to intermediate times. Interestingly, evolving the Wannier basis with respect to a dynamical Hartree-Fock Hamiltonian, thus accounting for interactions at the mean-field level leads to a substantial reduction of S for quite long times. Searching for an optimal entanglement cut by treating the translation-invariant Hermitian matrix \tilde{H}_t as a variational ansatz generating the basis transformation U_t [see Eq. (3)] [39], we are able to further reduce S significantly below the dynamical Hartree-Fock basis [see the inset of Fig. 1(b)] by using local optimization algorithms such as Gradient Descent and ADAM [42]. We now switch on $W > 0$ which is generally found to speed up the process of thermalization in 1D topological insulator models [43], thus allowing us to look at the long-time (close to equilibration) behavior of our model. For weak to modest interactions, we observe a quite remarkable universal aspect of entanglement in the long-time limit, namely, that S becomes largely independent of the choice of basis (see Fig. 2). This behavior exemplifies a quite generic mechanism that can be understood with the following physical picture [39]. When a system is quenched far from equilibrium by changing its gapped single-particle Hamiltonian, weak interactions are expected to lead to thermalization at an effective temperature β_e of the system with respect to the close to noninteracting postquench Hamiltonian. However, the thermal entropy of a free Hamiltonian [such as Eq. (4)] generically is independent (up to nonextensive boundary effects) on the basis of a bipartition with an average of $n_p/2$ particles in each subsystem. Thus, the basis dependence of the entanglement entropy in this scenario is a transient effect, even though it might last to long times. This basis independence in weakly interacting thermalizing insulators also affects the margin to be gained by entanglement minimization: By optimizing the aforementioned basis-change Hamiltonian \tilde{H}_t , starting from the set of Wannier orbitals in the long-time limit, here it is not possible to significantly reduce the entanglement entropy.

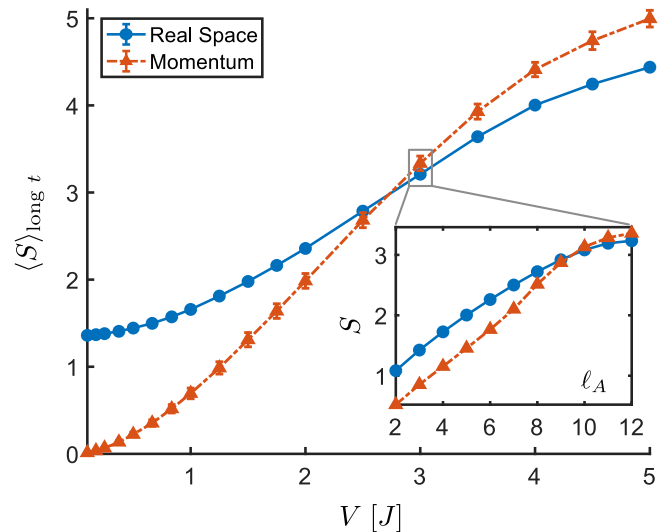


FIG. 3. Long-time average of S for the spinless Hubbard model (6) with $L = 24$, $\nu = 1/3$ as a function of the postquench next-nearest-neighbor interaction strength V . Inset: Scaling of S with the number of orbitals ℓ_A in A .

(ii) *Spinless NNN Fermi-Hubbard model.* As a second nonintegrable model system, we consider a spinless single-band Fermi-Hubbard model with a NNN interaction at filling $\nu = n_p/L$, defined by the Hamiltonian

$$H = \sum_j [-J(c_j^\dagger c_{j+1} + \text{H.c.}) + V(t)(n_j - \nu)(n_{j+2} - \nu)], \quad (6)$$

where J (fixed to 1 in the simulations) denotes the hopping strength, $n_j = c_j^\dagger c_j$, and $V(t) \geq 0$ represents the repulsive NNN interaction strength which is suddenly changed from 0 to a finite value over the quench at $t = 0$. We focus on $\nu = 1/3$ in the following, where the model (6) at zero temperature is known to stay in a metallic Luttinger liquid phase up to large $V > 0$ [44], and has been found to exhibit strongly ergodic behavior [45]. When comparing the long-time entanglement entropy of this model in real space and momentum space, we find an interesting basis dependence that persists even in the long-time limit: For weak to modest V , the long-time entanglement in momentum space is lower than in real space, whereas at strong correlations ($V \gtrsim 3J$), the real-space cut leads to lower entanglement entropy (see Fig. 3). This behavior may be interpreted as a dynamical manifestation of the generic competition between an interaction term that is diagonal in real space and a free band structure that is diagonal in momentum space in Hubbard models [39]. At short times, by contrast, entanglement for all V grows steeper in the momentum cut, owing to the nonlocal nature of the interaction in reciprocal space. In both cuts, entanglement clearly exhibits extensive (volume law) scaling for long times, as expected for an equilibrating ergodic system (see the inset of Fig. 3).

Concluding discussion. We conclude by putting our present results into a broader perspective from several angles. Generally speaking, nonintegrable ergodic systems are known to exhibit a generic dynamical behavior for the entanglement

entropy S in coherent quench dynamics starting from a weakly entangled (equilibrium) state: S initially grows linearly in time, reflecting a ballistic spreading of quantum information at a certain velocity [8–23]. At large times, close to thermalization, S approaches an extensive value (volume law), i.e., $S = \alpha V_A$, where V_A denotes the volume of subsystem A , since the entropy as an equilibrium thermodynamic potential is always extensive. While all of our present findings fit into this rough generic framework, here we identified and microscopically exemplified several general principles relating to the basis dependence and heterogeneous physical nature of dynamical entanglement growth.

First, for insulators with weak to modestly strong interactions that are quenched out of equilibrium by a change in their band structure, the transient entanglement exhibits a very strong basis dependence and may be reduced significantly beyond a dynamical mean-field solution by means of single-particle basis rotations. By contrast, the volume-law coefficient α of the long-time average of S becomes basis independent. This is because the system is thermalizing with respect to a nearly free Hamiltonian, and the thermal entropy for a free fermionic system typically is largely independent of the choice of bipartition, as long as each subsystem contains half of the degrees of freedom and accommodates on average half of the particles.

Second, in Hubbard models that are undergoing an interaction quench leaving the noninteracting Hamiltonian unchanged, a significant basis dependence of entanglement persists in the long-time limit, where the considered ergodic systems exhibit basis-dependent extensive entanglement scaling: Up to intermediate postquench interaction strengths entanglement is found to be weaker in reciprocal space while at stronger correlations the real-space cut has lower in S . This behavior dynamically reflects the competition between kinetic energy and interactions characteristic for Hubbard models.

These findings on distinguishing single-particle contributions to S from inherently more complex quantum correlations are not only of fundamental interest, but might also serve as important guidelines for the pursuit of devising more efficient numerical algorithms for quantum dynamics. Within the realm of thermal equilibrium, the observation that low-temperature states typically exhibit significantly lower (area-law [46,47]) entanglement than generic states has been crucial for systematically taming the exponential complexity of correlated

systems, e.g., with the advent of tensor-network methods [24–37], where the basis dependence of entanglement has been successfully exploited in the context of spin-boson models [48] and quantum chemistry settings [49–51]. However, far from equilibrium, generically the dynamical proliferation of entanglement eventually builds up an exponential wall even for the most powerful known computational methods. In this context, our results provide systematic insights addressing the question as to what extent both transient entanglement growth and long-time entanglement may be made computationally manageable, e.g., by extending tensor-network methods to a flexible representation of the physical degrees of freedom that allows for time-dependent basis choices.

In this Rapid Communication, we have been concerned with the influence of *single-particle* basis rotations on entanglement dynamics. At a conceptual level, our search for an optimal basis in which S is lowest may be interpreted as an entanglement-based dynamical mean-field approach aimed at minimizing the single-particle contributions to S . Thinking further along these lines, it is readily conceivable to consider more elaborate approximate solutions based on genuine many-body methods as a starting point for the choice of a *correlated* basis, which may eliminate even some higher-order quantum correlations from the system. Quantitatively exploring this approach and constructing hybrid numerical methods, where a physically motivated approximate solution serves as the starting point to be augmented by an unbiased tensor-network simulation, represents an interesting subject of future work.

Note added in proof. Recently, we became aware of two related papers [52,53]. The authors of Ref. [52] have applied the idea of a dynamical single-particle basis rotations on matrix product states (MPS), optimizing at each step a sequence of unitary two-site gates acting on the MPS. In Ref. [53], the authors have chosen the frequency basis as a computationally advantageous single-particle basis for a MPS transport calculation.

Acknowledgments. We acknowledge discussions with S. Barbarino, M. Hermanns, C. Mendl, and H.-H. Tu. L.P. and J.C.B. acknowledge financial support from the DFG through SFB 1143 (Project No. 247310070). Our numerical calculations were performed on resources at the TU Dresden Center for Information Services and High Performance Computing (ZIH).

-
- [1] X.-G. Wen, *Quantum Field Theory of Many-Body Systems* (Oxford University Press, Oxford, UK, 2007).
- [2] L. Amico, R. Fazio, A. Osterloh, and V. Vedral, *Rev. Mod. Phys.* **80**, 517 (2008).
- [3] M. A. Nielsen and I. L. Chuang, *Quantum Computation and Quantum Information* (Cambridge University Press, Cambridge, UK, 2000).
- [4] C. H. Bennett, G. Brassard, C. Crépeau, R. Jozsa, A. Peres, and W. K. Wootters, *Phys. Rev. Lett.* **70**, 1895 (1993).
- [5] M. B. Plenio and V. Vedral, *Contemp. Phys.* **39**, 431 (1998).
- [6] R. Horodecki, P. Horodecki, M. Horodecki, and K. Horodecki, *Rev. Mod. Phys.* **81**, 865 (2009).
- [7] T. Ono, R. Okamoto, and S. Takeuchi, *Nat. Commun.* **4**, 2426 (2013).
- [8] E. H. Lieb and D. W. Robinson, *Commun. Math. Phys.* **28**, 251 (1972).
- [9] P. Calabrese and J. Cardy, *J. Stat. Mech.* (2005) P04010.
- [10] G. De Chiara, S. Montangero, P. Calabrese, and R. Fazio, *J. Stat. Mech.* (2006) P03001.
- [11] A. M. Läuchli and C. Kollath, *J. Stat. Mech.* (2008) P05018.
- [12] H. Kim and D. A. Huse, *Phys. Rev. Lett.* **111**, 127205 (2013).
- [13] J. Schachenmayer, B. P. Lanyon, C. F. Roos, and A. J. Daley, *Phys. Rev. X* **3**, 031015 (2013).

- [14] J. S. Cotler, M. P. Hertzberg, M. Mezei, and M. T. Mueller, *J. High Energy Phys.* **11** (2016) 166.
- [15] W. W. Ho and D. A. Abanin, *Phys. Rev. B* **95**, 094302 (2017).
- [16] D. J. Luitz and Y. Bar Lev, *Phys. Rev. B* **96**, 020406(R) (2017).
- [17] M. Mezei and D. Stanford, *J. High Energy Phys.* **05** (2017) 065.
- [18] A. Nahum, J. Ruhman, S. Vijay, and J. Haah, *Phys. Rev. X* **7**, 031016 (2017).
- [19] A. Calzona, F. M. Gambetta, F. Cavaliere, M. Carrega, and M. Sassetti, *Phys. Rev. B* **96**, 085423 (2017).
- [20] S. I. Mistakidis, G. C. Katsimiga, P. G. Kevrekidis, and P. Schmelcher, *New J. Phys.* **20**, 043052 (2018).
- [21] C. W. von Keyserlingk, T. Rakovszky, F. Pollmann, and S. L. Sondhi, *Phys. Rev. X* **8**, 021013 (2018).
- [22] A. Nahum, J. Ruhman, and D. A. Huse, *Phys. Rev. B* **98**, 035118 (2018).
- [23] J. Surace, M. Piani, and L. Tagliacozzo, *Phys. Rev. B* **99**, 235115 (2019).
- [24] S. R. White, *Phys. Rev. Lett.* **69**, 2863 (1992).
- [25] S. Östlund and S. Rommer, *Phys. Rev. Lett.* **75**, 3537 (1995).
- [26] Y. Hieida, K. Okunishi, and Y. Akutsu, *New J. Phys.* **1**, 7 (1999).
- [27] F. Verstraete and J. I. Cirac, *Phys. Rev. A* **70**, 060302(R) (2004).
- [28] F. Verstraete and J. I. Cirac, [arXiv:cond-mat/0407066](https://arxiv.org/abs/cond-mat/0407066).
- [29] A. Daley, C. Kollath, U. Schollwöck, and G. Vidal, *J. Stat. Mech.* (2004) P04005.
- [30] F. Verstraete and J. I. Cirac, *Phys. Rev. B* **73**, 094423 (2006).
- [31] Y.-Y. Shi, L.-M. Duan, and G. Vidal, *Phys. Rev. A* **74**, 022320 (2006).
- [32] G. Vidal, *Phys. Rev. Lett.* **99**, 220405 (2007).
- [33] F. Verstraete, V. Murg, and J. I. Cirac, *Adv. Phys.* **57**, 143 (2008).
- [34] G. Vidal, *Phys. Rev. Lett.* **101**, 110501 (2008).
- [35] I. P. McCulloch, [arXiv:0804.2509](https://arxiv.org/abs/0804.2509).
- [36] L. Tagliacozzo, G. Evenbly, and G. Vidal, *Phys. Rev. B* **80**, 235127 (2009).
- [37] U. Schollwöck, *Ann. Phys.* **326**, 96 (2011).
- [38] A. Nauts and R. E. Wyatt, *Phys. Rev. Lett.* **51**, 2238 (1983).
- [39] See Supplemental Material at <http://link.aps.org/supplemental/10.1103/PhysRevResearch.1.012007> for technical details.
- [40] W. P. Su, J. R. Schrieffer, and A. J. Heeger, *Phys. Rev. Lett.* **42**, 1698 (1979).
- [41] A. J. Heeger, S. Kivelson, J. R. Schrieffer, and W. P. Su, *Rev. Mod. Phys.* **60**, 781 (1988).
- [42] D. P. Kingma and J. L. Ba, [arXiv:1412.6980](https://arxiv.org/abs/1412.6980).
- [43] A. Kruckenhauser and J. C. Budich, *Phys. Rev. B* **98**, 195124 (2018).
- [44] P. Schmitteckert and R. Werner, *Phys. Rev. B* **69**, 195115 (2004).
- [45] C. Neuenhahn and F. Marquardt, *Phys. Rev. E* **85**, 060101(R) (2012).
- [46] M. B. Hastings, *J. Stat. Mech.* (2007) P08024.
- [47] J. Eisert, M. Cramer, and M. B. Plenio, *Rev. Mod. Phys.* **82**, 277 (2010).
- [48] C. Guo, A. Weichselbaum, J. von Delft, and M. Voja, *Phys. Rev. Lett.* **108**, 160401 (2012).
- [49] A. O. Mitrushenkov, G. Fano, F. Ortolani, R. Linguerrì, and P. Palmieri, *J. Chem. Phys.* **115**, 6815 (2001).
- [50] S. Szalay, M. Pfeffer, V. Murg, G. Barcza, F. Verstraete, R. Schneider, and Ö. Legeza, *Int. J. Quantum Chem.* **115**, 1342 (2015).
- [51] M. Gluza, C. Krumnow, M. Friesdorf, C. Gogolin, and J. Eisert, *Phys. Rev. Lett.* **117**, 190602 (2016).
- [52] C. Krumnow, J. Eisert, and Ö. Legeza, [arXiv:1904.11999](https://arxiv.org/abs/1904.11999).
- [53] M. M. Rams and M. Zwolak, [arXiv:1904.12793](https://arxiv.org/abs/1904.12793).